Biogeosciences Discuss., 11, 16349–16389, 2014
www.biogeosciences-discuss.net/11/16349/2014/
doi:10.5194/bgd-11-16349-2014

Biogeosciences Discussions
Open Access

Large eddy simulations of surface roughness parameter sensitivity to canopy-structure characteristics

K. D. Maurer[1], G. Bohrer[1], and V. Y. Ivanov[2]

[1]Department of Civil, Environmental, & Geodetic Engineering, The Ohio State University, Columbus, OH, USA
[2]Department of Civil & Environmental Engineering, University of Michigan, Ann Arbor, MI, USA

Received: 15 October 2014 – Accepted: 23 October 2014 – Published: 27 November 2014

Correspondence to: G. Bohrer (bohrer.17@osu.edu)

Published by Copernicus Publications on behalf of the European Geosciences Union.

Abstract

Surface roughness parameters are at the core of every model representation of the coupling and interactions between land-surface and atmosphere, and are used in every model of surface fluxes. However, most models assume these parameters to be a fixed property of plant functional type and do not vary them in response to spatial or temporal changes to canopy structure. In part, this is due to the difficulty of reducing the complexity of canopy structure and its spatiotemporal dynamic and heterogeneity to less than a handful of parameters describing its effects of atmosphere–surface interactions. In this study we use large-eddy simulations to explore, in silico, the effects of canopy structure characteristics on surface roughness parameters. We performed a virtual experiment to test the sensitivity of resolved surface roughness to four axes of canopy structure: (1) leaf area index, (2) the vertical profile of leaf density, (3) canopy height, and (4) canopy gap fraction. We found roughness parameters to be highly variable, but were able to find positive relationships between displacement height and maximum canopy height, aerodynamic canopy height and maximum canopy height and leaf area index, and eddy-penetration depth and gap fraction. We also found negative relationships between aerodynamic canopy height and gap fraction, and between eddy-penetration depth and maximum canopy height and leaf area index. Using a decade of wind and canopy structure observations in a site in Michigan, we tested the effectiveness of our model-resolved parameters in predicting the frictional velocity over heterogeneous and disturbed canopies. We compared it with three other semi-empirical models and with a decade of meteorological observations. We found that parameterizations with fixed representations of roughness performed relatively well. Nonetheless, some empirical approaches that incorporate seasonal and inter-annual changes to the canopy structure performed even better than models with temporally fixed parameters.

BGD
11, 16349–16389, 2014

1 Introduction

Our ability to accurately predict mass and energy fluxes from the land surface to the atmosphere at any time scale depends on the accuracy of the surface drag parameterization (Finnigan, 2000; Mahrt, 2010). Over forested environments, vertical mixing of canopy air with the free atmosphere above, which is the process responsible for the exchange of energy, water vapor and CO_2 between the land surface and the atmosphere, is a function of the turbulent eddies created through interactions between vegetative structure (e.g., trees, tree-stems, leaves) and the wind (Thomas and Foken, 2007a). In many regional models, estimation of surface drag, and thus surface fluxes, is typically dependent upon parameterization of the friction velocity, u_*, based on Monin–Obukhov similarity theory (MOST) (Monin and Obukhov, 1954) using parameters that describe the effects of drag generated by the surface on the vertical distribution of wind speed. These parameters are displacement height, d, and roughness length, z_0. MOST is expected to be accurate high above the ground surface in the inertial sub-layer (ISL), where the viscous effects of the rough underlying surface may be neglected and the vertical flux of momentum is constant. The atmospheric layer directly above the rough surface, called the roughness sub-layer (RSL), typically fails to meet these criteria. Our understanding of aerodynamic properties near forest canopies within the RSL has led to higher order closure models (Raupach and Thom, 1981; Baldocchi and Meyers, 1989) and, as a result, empirical corrections for RSL dynamics have been added to the MOST model (Harman and Finnigan, 2007; De Ridder, 2010; Cellier and Brunet, 1992; Garratt, 1980; Mölder et al., 1999; Physick and Garratt, 1995; Raupach, 1992). These corrections allow us to utilize meteorological observation within the RSL, which is a typical limiting factor for eddy-covariance measurements across the globe.

In many land surface, vegetation, ecosystem, and hydrology models, such as the Community Earth System Model (CESM) (Gent et al., 2011), Mapping Evapotranspiration with Internalized Calibration (METRIC) (Allen et al., 2007), and

Surface Energy Balance Algorithm for Land (SEBAL) (Bastiaanssen et al., 1998), the surface sensible and latent heat fluxes are functions of the aerodynamic resistance for heat transfer, r_{ah}. r_{ah} is further parameterized as a function of the surface roughness parameters for momentum, d and z_0. In these models d and z_0 may be derived from different canopy structure characteristics. By the simplest approach, d and z_0 are linear function of site-level canopy height (h) – typically: $d \approx 0.66h$ (Cowan, 1968) and $z_0 \approx 0.10h$ (Tanner and Pelton, 1960). These estimates are limited, however, by the dynamic nature (space and time) of canopy structure characteristics. First, the canopy is a complex structure that is hard to describe using simple low-variable-number formulations. Second, estimates of the canopy structural characteristics are limited by the typical absence of data about the vertical distribution of leaf area (Massman and Weil, 1999; Shaw and Pereira, 1982) and tree-top heights, and the difference between coarse model grid-cell resolution and the fine-scale at which canopy structure characteristics vary and affect roughness and momentum and flux transfer.

One common approach to incorporate canopy structure in the parameterization of roughness length into models in a more realistic way utilizes satellite imagery products to estimate vegetation structure and relate it to canopy-roughness relationships. For example, a function based on the Normalized Difference Vegetation Index (NDVI) in the SEBAL model (Moran, 1990) or the Perrier Function (Perrier, 1982) used in the METRIC model. These canopy-roughness relationships have been shown to improve evapotranspiration estimates (Santos et al., 2012), but are specific to sparse or short vegetative environments, such as agricultural systems and are not typically recommended for forest environments (Bastiaanssen et al., 1998).

To incorporate the effects of canopy structure in denser and taller vegetative environments such as forests, empirical functions have been proposed using coarse canopy metrics such as canopy area index (the total, single-sided area of all canopy elements within a 1 m × 1 m ground area) (Raupach, 1994), stand density (stems per area), or leaf area index (LAI, the total surface area of leaves found within a 1 m × 1 m vertical column of vegetation) (Nakai et al., 2008a). However, the data required to use

BGD
11, 16349–16389, 2014

these functions are typically not available at most sites and, with the exception of LAI, are not yet obtainable through large-scale satellite remote sensing. In many climate models surface-layer grid cells are prescribed with biome-specific qualities, i.e., sets of parameters describing constant vegetation structure and flux-driving characteristics for all model cells containing a specific biome or plant functional type (PFT). For example, the Ecosystem Dynamic 2 (ED2, Medvigy et al., 2009) provides twenty different vegetation functional types, seven of which are representative of forested environments, to describe all land surfaces across the globe. Each such vegetation functional type is characterized by fixed canopy-height driven roughness parameters. Similarly, aerodynamic resistance to surface flux in the advanced hydrological model tRIBS+VEGGIE (Ivanov et al., 2008) is only driven by vegetation height, with is either prescribed, or set as a default per PFT.

Roughness parameters have been shown to scale with structure characteristics, such as the influence of area-index (vegetation area per ground area) terms on d and z_0 through numerical studies (Shaw and Pereira, 1982; Choudhury and Monteith, 1988) and wind-tunnel experiments (Raupach, 1994). Above-canopy meteorology data has shown estimates of roughness parameters to be highly variable both spatially and temporally (Maurer et al., 2013; Harman, 2012; Zhou et al., 2012). As evidence for canopy-roughness relationships has risen, various studies have attempted to generalize small-scale interactions between roughness parameters and canopy structure by deriving d and z_0 from above-canopy meteorological measurements (Braam et al., 2012; Maurer et al., 2013; Raupach et al., 1996; Nakai et al., 2008a), remote-sensing (Schaudt and Dickinson, 2000; Weligepolage et al., 2012), numerical experiments (Grimmond and Oke, 1999; Wouters et al., 2012), and large-eddy simulations (LES) (Aumond et al., 2013; Bohrer et al., 2009; Bou-Zeid et al., 2007, 2009). Although the understanding of these small-scale canopy-roughness interactions has grown, accounting for fine-scale canopy structure effects on roughness parameters in larger-scale climate models requires further development.

BGD
11, 16349–16389, 2014
LES of surface roughness parameters
K. D. Maurer et al.

In this study, we use the Regional Atmospheric Modeling System (RAMS)-based Forest Large-Eddy Simulation (RAFLES – Bohrer et al., 2008, 2009) for a virtual experiment to estimate the sensitivity of surface roughness parameters to specific characteristics of fine-scale canopy structure. Unlike most LES, RAFLES does not use a prescribed 2-D roughness length to calculate surface momentum fluxes or turbulent kinetic energy; instead RAFLES incorporates leaf-level drag heterogeneously in 3-D and dynamically in time based on a prescribed domain that includes the vegetation leaf density and stem diameters in each pixel (Chatziefstratiou et al., 2014). The details at which vegetation is represented in RAFLES make it particularly suitable for conducting this series of virtual experiments that simulate the drag parameters over a simplistic set of virtual canopy structures that vary in specific components of canopy structure, including stand density and patch fraction, canopy height, leaf area index and vertical profile of leaf density. The approach of prescribing drag in LES to resolve site-level roughness was previously tested and shown to provide higher accuracy than the traditional roughness parameterization (Aumond et al., 2013). Finally we use 10 years of direct observations of canopy structure and roughness parameters (Maurer et al., 2013) and compare five different approaches for representation of canopy structure in the modelled roughness parameters, including the one derived from our LES simulations, to estimate the sensitivity of modelled frictional velocity to temporal variation in roughness length.

2 Materials and methods

2.1 Theory

*

BGD
11, 16349–16389, 2014

Parameterization of aerodynamic canopy properties

Monin–Obukhov similarity theory (MOST) describes the relationships between the mean horizontal wind speed and the frictional velocity, which is a property of the turbulence of the flow, at all heights within the atmospheric surface layer (Monin and Obukhov, 1954). Further details on the formulation of MOST that was used in this work are described in Maurer et al. (2013). In brief, MOST relates surface stress to d and z_0 as

$$\frac{\kappa \overline{u_z}}{u_*} = \ln\left(\frac{z-d}{z_0}\right) - \psi_m\left(\frac{z-d}{L}\right) + \psi_m\left(\frac{z_0}{L}\right) + I\psi_u\left(\frac{z-d}{L}, \frac{z-d}{z_*-d}\right) \quad (1)$$

where $\overline{u_z}$ is the mean horizontal wind speed at height z, above the ground. Given the mean eastward and northward wind velocities, $\overline{u}$ and $\overline{v}$, $\overline{u_z}$ is rotated toward the wind direction such that

$$\overline{u_z} = \left(\overline{u}^2 + \overline{v}^2\right)^{1/2} \quad (2)$$

κ is the von Kármán constant, ~ 0.4, z_* is the upper limit of the RSL estimated as $2h$ (Mölder et al., 1999; Raupach et al., 1996), h is the canopy height. I is an indicator function defined as ($I = 1$ for $z \leq z_*$; or $I = 0$ for $z > z_*$). u_* is the friction velocity defined as

$$u_* = \left(\overline{u'w'} + \overline{v'w'}\right)^{1/2} \quad (3)$$

where each prime term (e.g., w') is the perturbation of the specific variable from its mean (e.g., $w - \overline{w}$). The atmospheric-stability correction function, $\psi_m(x)$, was described by Paulson (1970) for unstable atmospheric conditions ($z/L < 0$) as

$$\psi_m(x) = 2\ln\left[\frac{1+(1-16x)^{1/4}}{2}\right] + \ln\left[\frac{1+(1-16x)^{1/2}}{2}\right] - 2\tan^{-1}\left[(1-16x)^{1/4}\right] + \frac{\pi}{2} \quad (4)$$

BGD
11, 16349–16389, 2014

where x is either $(z-d)/L$ or z_0/L. The RSL correction, $\psi_u(x_1, x_2)$, was described by De Ridder (2010) as

$$\psi_u(x_1, x_2) = (1-16x_1)^{-1/4}\left[\left(1+\frac{\upsilon}{\mu \cdot x_2}\right)x_1\right]\frac{1}{\gamma}\ln\left(1+\frac{\gamma}{\mu x_2}\right)\exp(-\mu x_2) \quad (5)$$

where $x_1 = (z-d)/L$, $x_2 = (z-d)/(z_*-d)$, and υ, μ, and γ are empirical constants provided by De Ridder (2010) as 0.5, 2.59, and 1.5, respectively. The inclusion of the RSL correction ($\psi_u \neq 0$) occurs when the calculation is performed within the RSL ($z \leq z_*$, $I = 1$). Flux data is typically observed within the RSL at one point in space, requiring the implementation of the RSL correction. When conditions are neutrally buoyant, $(z-d)/L$ and z_0/L approach zero, and thus, $\psi_m(x)$ becomes negligible (Eq. 4).

Contrary to the classic estimate of z_0 (function of h), Thom (1971) suggested a relationship between z_0 and $(h-d)$, as opposed to a relationship between z_0 and h alone, where the ratio of $z_0/(h-d)$ was defined as λ – a dimensionless, stand-specific parameter. This allows z_0 to be dependent on the spacing of the surface roughness elements and not only their height as well. For example, $(h-d)$ will theoretically be smaller for more densely packed surfaces, providing a smoother surface and smaller roughness length. This relationship can be written as

$$z_0 = \lambda(h-d) \quad (6)$$

Nakai et al. (2008b) substituted the aerodynamic height, h_a, for the canopy height, h, into this relationship and rearranged the equation to read as

$$h_a = d + \frac{z_0}{\lambda} \quad (7)$$

Using Eq. (7) we can calculate simulation-specific λ values using h_a calculated from the horizontal wind profile and the empirically fitted d and z_0.

BGD
11, 16349–16389, 2014

We investigated the eddy penetration depth (δ_e), which is the length scale describing the vertical distance from the top of the canopy that is influenced by turbulent mixing from above. It is defined as the distance between h_a and the height where $\left(\overline{u_r'w'}\right)_h = 0.1\left(\overline{u_r'w'}\right)_{ha}$ (Nepf et al., 2007), where u_r is the downstream horizontal wind speed (i.e., $u_r = (u^2 + v^2)^{1/2}$) and each prime term (e.g., w') is the perturbation from the mean (e.g., $\overline{w} - w$).

2.2 Site description

The data used to test the effectivity of our LES-resolved, and other modeling approaches originates from a mixed, deciduous forest site at the University of Michigan Biological Station (UMBS) in northern, lower Michigan, USA (45°33′35″ N, 84°42′48″ W, elev. 236 m a.s.l.). The forest is dominated (~ 30 % of leaf area index) by early-successional bigtooth aspen (*Populus grandidentata*) and paper birch (*Betula papyrifera*), with a mean age of 85–90 years (Gough et al., 2013). The remaining leaf area is mostly represented by red oak (*Quercus rubra*), red maple (*Acer rubrum*) and white pine (*Pinus strobus*). Mean canopy height is roughly 20–25 m with an average stem density of ≈ 750 stems ha^{-1} (including only trees with DBH > 8 cm). Eddy covariance flux measurements have been ongoing at the site since 1999 and data is available through AmeriFlux (http://ameriflux.lbl.gov/), site code: US-UMB. Empirical allometic equations, fitted to measurements in this site (Garrity et al., 2012) are used to determine canopy height from a tree census and measurements of diameter at breast height (DBH). Full censuses were conducted in 2001 and 2010, and partial censuses of DBH, over hundreds of trees, are measured every year. Leaf area index is measured weakly using an optical sensor (LAI2000, Licor Biosciences, Lincoln, NE, USA). More details on the calculation of roughness length parameter from wind observations in the site and the determination of canopy structure are described in Maurer et al. (2013).

BGD
11, 16349–16389, 2014

LES of surface roughness parameters

K. D. Maurer et al.

Portable canopy lidar measurements (Hardiman et al., 2013) where used to determine the mean leaf area density profile that was used as the "natural" leaf area density case.

2.3 Large eddy simulations

We used wind fields and heat fluxes from RAFLES simulations results to calculate surface roughness parameters of simplified virtual forests. RAFLES (Bohrer et al., 2009) resolves the canopy as a 3-D heterogeneous domain where the leaves interact with the flow inside the simulation domain. In each grid cell within the canopy sub-domain, the canopy is represented as leaf density and volume restriction terms. The leaf density determines the drag force that is applied to wind flow through that grid cell. It is combined with radiation attenuation (given the leaf densities in the grid cells above) to determine the sensible and latent heat fluxes emitted in each grid cell. The model uses the finite volume approach for discretization of the simulation domain. It resolves the effects of volume restriction due to the volume of the vegetation (stems, branches) by reducing the aperture areas available for flux exchange between each pair of neighboring grid cells and by reducing the volume that is available for flow within each grid cell according to the volume of the vegetation present within the grid cell (Chatziefstratiou et al., 2014).

Simulations consisted of three hours of simulation time at a time step of 0.02 s. RAFLES uses a nested time stepping scheme with higher frequency calculations for turbulence and further higher for pressure perturbations. Eight pressure and four turbulence time steps were nested in one model time step. Output data snapshots of all grid cells in the simulation domain were recorded every 2 s. The initial 2.5 h of simulation time were used as a "spin-up" period to ensure satisfactory turbulent mixing and semi-stability of the vertical profiles of turbulence and potential temperature. The latter half hour of simulation time was used for analysis, consisting of 300 2 s snapshots. Flux and wind statistics were calculated as perturbations from their instantaneous horizontal spatial means. These statistics were then integrated over the

BGD
11, 16349–16389, 2014

300 2 s snapshots to compile one 30 min block average of fluxes and wind statistics per simulation.

Synthetic virtual domains covered 1.25 km × 1.25 km × 1.4 km (length × width × height) at a horizontal grid spacing of 5 m × 5 m, which approximately corresponds to the mean size of individual tree-crowns. Vertical grid spacing was 3 m in the lower sub-domain, from the ground to 100 m a.g.l. Above that region we gradually increased of the vertical grid spacing by 12 % per each subsequent layer up to a maximal grid spacing of 30 m. The vertical grid spacing then remained constant above that height up to the model top at 1.4 km. The model has periodic boundary conditions at the lateral boundaries, no-slip boundary conditions at the bottom boundary and a reflective top boundary with Rayleigh friction to dampen vertical perturbations at the top 6 model layers (180 m). Initial conditions were horizontally homogeneous and followed a prescribed vertical profile for potential temperature, humidity, and wind speed. Surface boundary layer height was prescribed by the shape of the potential temperature profile. Latent and sensible heat fluxes were prescribed based on observed mean noontime observations for August 2011 above the canopy at US-UMB. For each column at the horizontal simulation domain, the sum of the fluxes and Bowen ratio were distributed around the prescribed mean as an empirical function of LAI. Fluxes were further distributed vertically following a leaf-area dependent empirical exponential profile. More details on the numerical setup of the model and the approach for flux forcing are provided in Bohrer et al. (2009).

2.4 Virtual experiment setup: sensitivity analysis to quantify the effects of specific canopy-structure characteristics on roughness parameters

Forest canopies are a complex array of 3-D structures. Many of these structural characteristics affect the airflow inside and above the canopy and, consequently, affect the resulting roughness parameters and surface-aerodynamic properties that describe such canopy structure. Using synthetic cases representing different aspects of canopy structure we conducted a virtual experiment to test the sensitivity of roughness parameters to four axes of canopy structure: (1) mean site-level LAI, (2) vertical leaf area density (LAD, $m^2\,m^{-3}$) profile, (3) canopy height, and (4) canopy patch-level continuity (gap fraction). These four axes were individually varied from: (1) LAI: 1.0, 2.6, 3.2, 3.7, and 4.2 $m^2\,m^{-2}$, (2) mode of LAD profile: "Lower", "Middle", "Upper", and "Natural" (see Fig. A1), (3) canopy height: 9, 15, 21, and 27 m, (4) gap fraction: 0, 10, 25, 35, and 50 % (see Fig. A2).

In the gap fraction cases, canopy gaps were randomly created across the domain ranging from a single-pixel (25 m^2, tree-crown scale) to multi-pixel blocks (tens to hundreds m^2). A gap was described by shorter vegetation ($h = 9$ m) and a non-gap (closed canopy) was described by taller vegetation ($h = 27$ m). It should be noted that we introduced gaps in our horizontally homogenous canopy using holes of varying sizes and shapes, which was done to minimize the complexity of the prescribed "heterogeneity" treatment. However, this practice may not have been well-representative of actual, heterogeneous canopy environments with tree-fall gaps. Changes along the four canopy-structure axes yielded twenty permutation cases. A list of all simulation cases and the canopy-structure characteristics is presented in Table 1.

2.5 Empirical determination of roughness parameters from simulations results

We determined the effective aerodynamic canopy height, h_a, by identifying the height at which the inflection point between the sub-canopy and above-canopy horizontal wind profiles (Thomas and Foken, 2007b). To find this point we compiled a domain-averaged horizontal wind-speed profile by finding the spatial mean rotated wind speed, h_r, at each vertical layer of the domain for the 30 min simulation period analyzed using Eq. (2) with each vertical model layer height r substituting the physical height z. As RAFLES was able to estimate wind statistics across a large domain, we fit the wind profile in space using data within and above (Eq. 1, $I = 1$, $I = 0$, respectively) the RSL when calculating the LES-derived roughness parameters. We then interpolated a curve through these points and found the height above the ground where the second derivative of the horizontal wind profile was equal to zero. Next, the vertical profile of horizontal mean wind speed from vertical layers above h_a and below 95 m above ground (above which level the lateral forcing of wind speed was effective) was fitted to Eq. (1) to determine d and z_0 using the friction velocity and Obukhov length within the ISL. The empirical fit was calculated using MATLAB's (version R2013b, The MathWorks, Inc., Natick, MA, USA) nonlinear, least-squares fit function: *fit*( ). The domain-averaged u_* and Obukhov length were calculated for each vertical layer and the mean u_* and Obukhov length found within the ISL were used. We constrained the fit solution for the surface roughness parameters to a meaningful range by limiting d to be between 0 and h_a of the simulated forest and z_0 to be larger than 0.

2.6 Surface roughness parameters: forest structure effects

Using the results of our simulations with ranges of virtual canopies we determined which of the specific canopy structure features, if any, had significant effects on individual roughness parameters and eddy penetration depth through a 3-way ANOVA test. Here we tested the effects of (1) maximum canopy height, (2) LAI, and (3) gap fraction on the suite of simulations with "Natural" vertical LAD profiles (we ignored the three "unnatural" simulations with "Upper", "Middle", and "Lower" LAD profiles because there the effect of LAD position on any roughness parameter was chaotic). Maximum canopy height was used instead of mean canopy height because maximum canopy height was more tightly correlated to each roughness parameter than mean canopy height.

2.7 Testing empirical models linking roughness parameters to biometric measurements

Results of our virtual experiment provide relationships between easily measurable characteristics of the canopy (i.e., LAI and maximum canopy height) and roughness parameters. We name this parameterization approach (a) "Biometric" and discuss it at detail in the results Sect. 3.2. We evaluated the potential improvement to surface flux estimates using these relationships and compared this improvement with modeled u_* values using alternative common approaches. Numerous past studies have attempted to derive relationships between roughness parameters and canopy-structure statistics. We chose two in this study for comparison with our observations and simulation-derived approach: (b) Raupach (1994) calculated d and z_0 as functions of canopy area index (Λ), drag coefficient (c_d), and canopy height (h):

$$d = \left[1 - \frac{1 - \exp\left(-\sqrt{2c_\mathrm{d}\Lambda}\right)}{\sqrt{2c_\mathrm{d}\Lambda}}\right] h \quad (8)$$

and

$$z_0 = \left[\left(1 - \frac{d}{h}\right)\exp\left(-\frac{\kappa\overline{u}}{u_*} - \eta_h\right)\right] h \quad (9)$$

where $c_d = 7.5$, $\eta_h = 0.193$, and $\Lambda = 2nbh/A$, where n is the number of stems, b is the mean diameter at breast height, h is the mean tree height, and A is the total ground area within the sampling area. Alternatively, (c) Nakai et al. (2008a) calculated d and z_0 as functions of stand density (ρ_s), LAI, and h:

$$d = \left[1 - \left(\frac{1 - \exp(-\alpha\rho_\mathrm{s})}{\alpha\rho_\mathrm{s}}\right)\left(\frac{1 - \exp(-\beta\mathrm{LAI})}{\beta\mathrm{LAI}}\right)\right] h \quad (10)$$

and

$$z_0 = 0.264\left(1 - \frac{d}{h}\right) h \quad (11)$$

where α and β are 7.24×10^{-4} ha stems^{-1} and 0.273, respectively, and we used the US-UMB stand density of 750 stems ha^{-1}.

BGD
11, 16349–16389, 2014
LES of surface roughness parameters
K. D. Maurer et al.

We evaluate the resulting frictional velocity of all these structure-driven parameterization approaches using 30 min observed values of u_*, canopy height and LAI over multiple years at US-UMB (2000–2011, 34 m a.g.l.). We compared the accuracy of these approach with the accuracy of u_* estimates from four other direct empirical methods, all of which use Eq. (1) forced with the same decadal dataset of observed $\overline{u}$ and L, (Maurer et al., 2013) but with roughness parameter inputs determined using: (1) "Yearly Observed" – growing season d and z_0 observed during each year at US-UMB from 2000–2011, (2) "Classical" – $d = 0.66h$ and $z_0 = 0.10h$, where we use $h = 22$ m, (3) the third class of model included in this comparison where the three (a–c) structure-driven approaches listed above.

Modeled u_* was regressed against observed u_* and the slope of the fit, coefficient of determination (r^2), and coefficient of variation (CV; ratio of standard error to mean measured u_*) were reported. For the "Yearly Observed" method we tested the ability to use the observed roughness parameters of any single year to estimate long-term friction velocity. Roughness parameters for each year (2000–2011) were input into Eq. (1), resulting in 12 separate friction velocity models. We reported the slope of the fit, r^2, and CV for the mean of all 12 models, the most accurate year's model (2008), and the least accurate year's model (2005). The "Classical" method used one value for d and z_0 across the 12 years of data, while the structure-driven methods (Sect. 2.7, approaches a–c) have a unique estimate for roughness parameters each year based on their corresponding structure inputs for the specific year. Because "Yearly Observed" roughness parameters were calculated for neutral to slightly unstable atmospheric conditions during daytime in the growing season, we only used data corresponding to these specific time and atmospheric conditions.

BGD
11, 16349–16389, 2014

3 Results

3.1 Virtual experiment to explore canopy-roughness relationships

We found that d was significantly affected by maximum canopy height (h_{max}) (3-way ANOVA, Table 2). We also found that h_a and δ_e were significantly affected by h_{max}, LAI, and gap fraction (GF) (Table 2). z_0 was not found to be significantly affected by any single aspect of canopy structure investigated within this study. As suggested by Thom (1971) and Nakai et al. (2008b) we checked the relationship between z_0 and ($h_a - d$) and found a significant relationship ($r^2 = 0.72$, $P < 0.001$).

We found a positive relationship between d and h_{max} ($d = 0.69h_{max}$ – fit forced through [0,0], Fig. 1). Surprisingly, canopy gaps showed little effect on d, as a higher correlation existed between d and h_{max} ($r^2 = 0.78$) than between d and mean canopy height ($r^2 = 0.48$) across the gap fraction sensitivity analysis. There was little change to d with increasing gap fraction; therefore, the relationship with h_{max} (which was constant as the number of gaps increased) was selected instead of mean canopy height (which decreased as the number of gaps increased). Seasonality (leaf-on vs. leaf-off) also showed surprisingly small differences in d as height was varied, which had previously been observed at US-UMB (Maurer et al., 2013).

We found positive h_a–h_{max} and h_a–LAI relationships and a negative h_a–gap fraction (GF) relationship (Fig. 2). We note that a positive h_a–h relationship was previously observed at US-UMB using 12 years of meteorological data and tree-growth censuses (Maurer et al., 2013). By utilizing the suite of RAFLES simulations we empirically fit a single canopy–h_a relationship as

$$h_a = h_{max} + a\text{LAI} + b\text{GF} + c \quad (12)$$

where $a = 0.06$ m, $b = (-)0.69$ m, and $c = (-)0.11$ m.

We found a negative δ_e–LAI relationship and positive δ_e–h_{max} and δ_e–GF relationships (Fig. 3). As expected, we found δ_e to be consistently higher during leaf-off periods compared to leaf-on periods at corresponding heights and gap fractions as wind was better able to penetrate the sub-canopy. Increased LAI intensified the effect of gap fraction on δ_e as the slope of the leaf-on fit was larger than that of leaf-off periods. By utilizing the suite of RAFLES simulations we empirically fit a single canopy-δ_e relationship as

$$\delta_e = h_{max} + a\mathrm{LAI} + b\mathrm{GF} + c \quad (13)$$

where $a = (-)1.07$ m, $b = 0.41$ m, and $c = (-)6.89$ m.

Relationships were empirically fit using roughness parameters from each RAFLES simulation except for those with "unnatural" vertical LAD profiles (i.e., "Upper", "Middle", "Lower") as no patterns were observed between any roughness parameters and vertical LAD profile. A full list of roughness parameters for each simulation may be found in Table A1.

3.2 Canopy-roughness improvements to surface flux models

Using the h–h_{max} relationship found from the virtual experiment, we empirically fit the "Biometric" h_a using Eq. (11). We input a gap fraction of 5 %, which was found by calculating the percent area within the NCALM lidar scan domain with vegetation less than 2 m, and the peak site-level LAI measured at US-UMB each year from 2000 to 2011 (Maurer et al., 2013). "Biometric" d and z_0 were calculated using the d–h_{max} and z_0–$(h_a - d)$ relationships from the virtual experiments. The d–h_{max} and z_0–$(h_a - d)$ relationships used were

$$d = 0.69h_{max} \text{ and } z_0 = \lambda(h_a - d) \quad (14)$$

where λ was empirically determined through the virtual sensitivity experiment to be 0.34.

We found each of the 12 "Yearly Observed" models to be more accurate than the u_* model produced using the "Classical" method (Table 3). Model bias (estimated by the slope of the modeled vs. observed fit line, were 1 indicates no bias) of the worst "Yearly

BGD
11, 16349–16389, 2014

Observed" model (slope = 1.59) was lower than the "Classical" method (slope = 1.63), while the best "Yearly Observed" model had a slope of 1.02 %. The coefficient of variation (CV – the ratio of SD to the mean) of the worst "Yearly Observed" model was lower (CV = 27 %) than the "Classical" method (CV = 28 %), while the best "Yearly Observed" model had a CV of 3 %.

Of the canopy-roughness methods, the "Raupach 94" functions (Eqs. 7 and 8) performed the best (slope = 1.32, $r^2 = 0.80$, CV = 18 %) and was more accurate than the mean of all 12 Yearly Observed models (slope = 1.38, $r^2 = 0.80$, CV = 20 %). Our "Biometric" functions (Eqs. 11, 13 and 14, slope = 1.64, $r^2 = 0.80$, CV = 28 %) did not add any more predictive power than the "Classical" method. The "Nakai 08" functions (Eqs. 9 and 10) proved to be incompatible with our site and was unable to capture the canopy-roughness relationships specific to our forest.

4 Discussion

4.1 Response of roughness parameters to canopy structure change

We found that the aerodynamic canopy height (h_a) is sensitive to canopy structure and is linearly scaling with leaf area, canopy height and gap fraction (Fig. 2). Similarly eddy penetration depth was affected by canopy structural characteristics, while the classical roughness parameters, z_0 and d, were less sensitive to canopy characteristic, and the only significant relationship we found was between d and h_{max} (Fig. 1). Our simulations did not detect a continuous increase to d or z_0 with LAI, which was inconsistent with several previous wind tunnel or model studies (Choudhury and Monteith, 1988; Grimmond and Oke, 1999; Raupach, 1994; Shaw and Pereira, 1982). We suggest that this was due to sensitivity of the values of z_0 and d to the wind profile, which leads to tradeoffs between the two, such that similar solutions can be fit either with low d and high z_0, or vice versa. Maurer et al. (2013) observed similar variations and tradeoffs in observed z_0 and d values. Nonetheless, In deciduous canopies, the relationship between roughness parameters and LAI may be attributed to eddy-penetration depth (Shaw et al., 1988). As LAI increases, the ability for eddies to transport momentum deep into the canopy is weakened (Fig. 3a). We saw this phenomena within our study, as weaker sub-canopy wind speed and turbulence corresponded to higher LAI (Fig. 4). We hypothesized that a decrease in δ_e with LAI would result in an increase in d and a decrease in z_0. However, d and z_0 in our study were much more irregular, suggesting that d and z_0 are driven by additional aerodynamic-canopy property than δ_e.

The lack of seasonal differences in roughness parameters (i.e., leaf-off vs. leaf-on) within the virtual sensitivity experiment may suggest that leaf area is not the primary driver of previously found seasonal differences in roughness parameters. The seasonal differences in climate (Lindroth, 1993) and thermal stability (Dupont and Patton, 2012; Harman, 2012; Shaw et al., 1988; Zhou et al., 2012) may in fact be the primary drivers. As measurements leading to significant differences in roughness parameters across seasons at US-UMB (Maurer et al., 2013) also encountered these seasonal differences in climate and thermal stability, it is possible that seasonal variability in environmental forcing plays a larger role than canopy structure at US-UMB. A second possible explanation behind the lack of roughness parameter seasonality could be that our "leaf-off" LAI value of 1.0 $m^2\,m^{-2}$ may be too high.

We found positive d–h_{max} and h_a–h_{max} relationships independent of LAI. A strong correlation had previously been reported between h_a and h (Nakai et al., 2008b; Bohrer et al., 2009; Maurer et al., 2013; Thomas and Foken, 2007b). As canopy height was the only variable changed in the roughness-height portion of our sensitivity study, it is reasonable to assume that δ_e would be relatively constant, regardless of canopy height. However, as canopy height increased within our virtual domain the constant mean site-level LAI was stretched further in the vertical direction. Therefore, the total leaf density in the upper canopy was smaller for taller canopies resulting in an increased δ_e with canopy height (Fig. 3b). In spite of increased δ_e, we also observed a positive d–h_{max} relationship. This was likely driven by the less than a 1 : 1 relationship between δ_e and

BGD
11, 16349–16389, 2014

canopy height, allowing for the increase to d with canopy height, which also had less than a 1 : 1 relationship.

We found a linear relationship between h_a and gap fraction. However, the lack of any relationships between roughness parameters and gap fraction was surprising, as Bohrer et al. (2009) found increases to d, z_0, and h_a in patchier canopies (more gaps) during leaf-on conditions. Unlike the heterogeneous canopies used in the Bohrer et al. (2009) study, our virtual canopy was, by design, a horizontally homogenous with holes of varying sizes and shapes. This was done in order to minimize the complexity of the prescribed "heterogeneity" treatment but may not have been well-representative of actual, heterogeneous canopy environments with tree-fall gaps. Also, the scale of the gaps prescribed here, corresponding with 1–2 crown sizes was typically smaller than those in the Bohrer et al. (2009) experiments.

Intuitively, increased gap fraction led to increased δ_e regardless of season, as more canopy openings allowed wind to penetrate deeper into the canopy. Eddy-penetration depth was consistently larger during leaf-off periods compared to leaf-on periods, while the presence of higher LAI resulted in larger shifts in δ_e as gap fraction was increased (Fig. 3c). These findings are not surprising, as Shaw et al. (1988) found deeper δ_e at lower LAI. The presence of gaps creates changes to the horizontal wind profile, a driver of surface fluxes. For example, we found that increased gap fraction corresponded to increased sub-canopy turbulence and horizontal wind speed, but also weaker above-canopy turbulence and horizontal wind speed (Fig. 5a and b). This was likely due to the extension of turbulent eddy penetration deep into canopy gaps (Fig. 5c), which is less likely to occur in horizontally homogenous canopies (Fig. 5d–f). The presence of canopy gaps also introduces more "wake" environments (downwind gaps immediately following structural elements) which have been shown to experience significantly different aerodynamic properties than neighboring "non-wake" environments (Böhm et al., 2013).

We found no significant correlations between roughness parameters and the mode of the vertical LAD profile, as the variability in roughness parameters over the range

BGD
11, 16349–16389, 2014

of LAD scenarios was extremely high (Table A1). Shaw and Pereira (1982) showed variable interactions between roughness parameters and the mode of the vertical LAD profile at constant site-level LAI: (1) d increased as the majority of leaves moved vertically from the bottom of the canopy to the upper layers of the canopy (i.e., more like our "Upper" LAD profile than "Middle" or "Lower") and (2) at low (high) site-level LAI, z_0 increased (decreased) as the majority of leaves moved vertically from the bottom of the canopy to the upper layers. The inclusion of the LAD profile into a basal-weighted estimate of canopy height has also been shown to have a stronger relationship with h_a, as compared to the h_a–h relationship (Nakai et al., 2010). In this study we found no consistent canopy-wind or canopy-turbulence relationships involving the vertical LAD profile (Fig. 6).

Although a portion of the change to roughness parameters may be attributed to the effects of the LAD profile, incorporation of this canopy-structure characteristic into models is complicated due to the difficulty in accurately measuring the LAD profile. A major challenge is the saturation effect on remote sensing products in the presence of high LAI (e.g., Parker et al., 2004) and scaling such inferences to the site level. Additionally, LAD profiles may change in complex ways across the landscape and over many time scales (seasons, years, decades) due to disturbance or senescence. As our virtual experiment has shown, the effects of the vertical LAD profile are inconsistent with a simple representation of the vertical distribution of LAD using its vertical bias as a single descriptive characteristic. Site-level mean LAI is easier to measure and, in general, a more reliable characteristic of canopy structure. Therefore, incorporating changes to LAI over time is likely to be more effective when predicting its effects on roughness parameters.

4.2 Integrating canopy-structure characteristics into flux models

In the worst case, the "Yearly Observed" model demonstrated 5 % less error than the "Classical" canopy-roughness relationships (CV = 27 % vs. CV = 28 %). On average the "Yearly Observed" model had 30 % less error (CV = 20 %), while the best case had 91 % less error (CV = 3 %). The low spatial coverage by flux networks over the globe limits the use of this method across large spatial domains. In addition, previous observation studies were unable to find stable, long-term trends of d and z_0 over time (Maurer et al., 2013). From both a spatial and temporal perspective, biometric observations may be the most reliable method to estimate long-term roughness parameters. Our ability to estimate LAI over a broad range of spatial and temporal scales is continuously improving through the use of on-site biometric measurements, remote sensing, and satellite observations (Chen et al., 2002; Jonckheere et al., 2004; Zheng and Moskal, 2009).

Variable success by the three canopy-roughness methods may not be surprising, as a study by Grimmond and Oke (1999) determined that careful consideration must be given to surface height, complexity, and density when selecting an empirical method based on surface characteristics to calculate roughness parameters. In their urban study of building heterogeneity, Grimmond and Oke (1999) suggested the method of Raupach (1994) for random building arrangements, which may provide insight towards its success in this study over our heterogeneous forest canopy. Similar reasoning could provide insight towards the poor performance of the method of Nakai et al. (2008a) at US-UMB, which is less dense, taller, and has higher LAI than those sites used to parameterize the "Nakai 08" method.

The "Biometric" method presented in this study is essentially the "Classical" method, with the major difference being the use of maximum canopy height (with small perturbations based on LAI and gap fraction) as opposed to mean canopy height. The result being that maximum canopy height does not model friction velocity any better than mean canopy height at US-UMB. More detailed, or different, canopy-structure characteristics are likely necessary for model improvement. Care must be used when selecting a canopy-roughness relationship at each site, as the roughness-structure dynamics of a specific forest may not transfer to another, regardless of similarities in stand age, structure, species composition, or climate. Further investigation to validate

BGD
11, 16349–16389, 2014
LES of surface roughness parameters
K. D. Maurer et al.

canopy-roughness relationships across a suite of sites, and spatial and temporal resolutions is required.

5 Conclusions

In this study we used an LES, long-term meteorological observations, and remote sensing of the forest canopy to explore the effects of canopy structure on surface roughness parameters. We performed a virtual experiment to test the sensitivity of roughness parameters with respect to four axes of variation in canopy structure: (1) leaf area index, (2) the mode of the vertical profile of LAD, (3) canopy height, and (4) gap fraction. We found consistent relationships between roughness parameters and LAI, maximum height, and gap fraction. We call for awareness of the significant effects that canopy structure has on surface fluxes. Many easily obtainable metrics of canopy-roughness properties are available through a suite of measurements, such as on-site meteorological and biometric observations or satellite-derived site characteristics. Additionally, many ecosystem models and ecosystem modules within earth system models resolve the growth of the forest and accurately predict canopy height and LAI. The canopy structure data could be used to dynamically affect the roughness-length parameterization in the models and improve surface flux modeling. Due to limited spatial coverage by direct meteorological measurements, remote sensed structure statistics, and stand inventories, we suggest utilizing site- and time-specific biometric measurements of canopy structure to estimate site-level d and z_0. The effectivity of these model improvements will, of course, be dependent upon the quality, quantity, and resolution of the datasets available at the forest of interest.

Acknowledgements. We thank Peter Curtis and Christoph Vogel for running the AmeriFlux US-UMB and US-UMd flux sites and FASET, and for advice in conducting this study. We thank Brady Hardiman for the use of LiDAR data provided through an NSF–NCALM graduate seed award. This research was supported by the U.S. Department of Energy's Office of Science, Office of Biological and Environmental Research, Terrestrial Ecosystem Sciences program under Awards No. DE-SC0 006 708 and DE-SC0 007 041 and the Ameriflux Management project under Flux Core Site agreement No. 7 096 915 through Lawrence Berkeley National Laboratory, and additional support by the National Science Foundation grant DEB-0 911 461, and the National Oceanic and Atmospheric Administration award NA11OAR4 310 190. KDM was funded in part by an NSF IGERT Fellowship DGE-0 504 552 awarded through the UMBS Biosphere–Atmosphere Research Training (BART) program. Any opinions, findings, and conclusions expressed in this material are those of the authors and do not necessarily reflect the views of the National Science Foundation or the Department of Energy.

References

Allen, R., Tasumi, M., Morse, A., Trezza, R., Wright, J., Bastiaanssen, W., Kramber, W., Lorite, I., and Robison, C.: Satellite-based energy balance for mapping eapotranspiration with iternalized clibration (METRIC) – applications, J. Irrig. Drain. E.-ASCE, 133, 395–406, doi:10.1061/(ASCE)0733-9437(2007)133:4(395), 2007.

Aumond, P., Masson, V., Lac, C., Gauvreau, B., Dupont, S., and Berengier, M.: Including the drag effects of canopies: real case large-eddy simulation studies, Bound.-Lay. Meteorol., 146, 65–80, doi:10.1007/s10546-012-9758-x, 2013.

Baldocchi, D. D. and Meyers, T. P.: The effects of extreme turbulent events on the estimation of aerodynamic variables in a deciduous forest canopy, Agr. Forest Meteorol., 48, 117–134, doi:10.1016/0168-1923(89)90011-7, 1989.

Bastiaanssen, W. G. M., Menenti, M., Feddes, R. A., and Holtslag, A. A. M.: A remote sensing surface energy balance algorithm for land (SEBAL). 1. Formulation, J. Hydrol., 212–213, 198–212, doi:10.1016/S0022-1694(98)00253-4, 1998.

Böhm, M., Finnigan, J. J., Raupach, M. R., and Hughes, D.: Turbulence structure within and above a canopy of bluff elements, Bound.-Lay. Meteorol., 146, 393–419, doi:10.1007/s10546-012-9770-1, 2013.

Bohrer, G., Nathan, R., Katul, G. G., Walko, R. L., and Avissar, R.: Effects of canopy heterogeneity, seed abscission, and inertia on wind-driven dispersal kernels of tree seeds, J. Ecol., 96, 569–580, doi:10.1111/j.1365-2745.2008.01368.x, 2008.

Bohrer, G., Katul, G. G., Walko, R. L., and Avissar, R.: Exploring the effects of microscale structural heterogeneity of forest canopies using large-eddy simulations, Bound.-Lay. Meteorol., 132, 351–382, doi:10.1007/s10546-009-9404-4, 2009.

Bou-Zeid, E., Parlange, M. B., and Meneveau, C.: On the parameterization of surface roughness at regional scales, J. Atmos. Sci., 64, 216–227, doi:10.1175/JAS3826.1, 2007.

Bou-Zeid, E., Overney, J., Rogers, B. D., and Parlange, M. B.: The effects of building representation and clustering in large-eddy simulations of flows in urban canopies, Bound.-Lay. Meteorol., 132, 415–436, doi:10.1007/s10546-009-9410-6, 2009.

Braam, M., Bosveld, F., and Moene, A.: On Monin-Obukhov scaling in and above the atmospheric surface layer: the complexities of elevated scintillometer measurements, Bound.-Lay. Meteorol., 144, 157–177, doi:10.1007/s10546-012-9716-7, 2012.

Cellier, P. and Brunet, Y.: Flux-gradient relationships above tall plant canopies, Agr. Forest Meteorol., 58, 93–117, doi:10.1016/0168-1923(92)90113-I, 1992.

Chatziefstratiou, E. K., Velissariou, V., and Bohrer, G.: Resolving the effects of aperture and volume restriction of the flow by semi-porous barriers using large-eddy simulations, Bound.-Lay. Meteorol., 152, 329–348, doi:10.1007/s10546-014-9923-5, 2014.

Chen, J. M., Pavlic, G., Brown, L., Cihlar, J., Leblanc, S. G., White, H. P., Hall, R. J., Peddle, D. R., King, D. J., Trofymow, J. A., Swift, E., Van der Sanden, J., and Pellikka, P. K. E.: Derivation and validation of Canada-wide coarse-resolution leaf area index maps using high-resolution satellite imagery and ground measurements, Remote Sens. Environ., 80, 165–184, doi:10.1016/S0034-4257(01)00300-5, 2002.

Choudhury, B. J. and Monteith, J. L.: A four-layer model for the heat budget of homogeneous land surfaces, Q. J. R. Meteorol. Soc., 114, 373–398, doi:10.1002/qj.49711448006, 1988.

Cowan, I. R.: Mass, heat and momentum exchange between stands of plants and their atmospheric environment, Q. J. R. Meteorol. Soc., 94, 523–544, doi:10.1002/qj.49709440208, 1968.

De Ridder, K.: Bulk transfer relations for the roughness sublayer, Bound.-Lay. Meteorol., 134, 257–267, doi:10.1007/s10546-009-9450-y, 2010.

Dupont, S. and Patton, E. G.: Influence of stability and seasonal canopy changes on micrometeorology within and above an orchard canopy: The CHATS experiment, Agr. Forest. Meteorol., 157, 11–29, doi:10.1016/j.agrformet.2012.01.011, 2012.

Finnigan, J.: Turbulence in plant canopies, Annu. Rev. Fluid Mech., 32, 519–571, 2000.

Garratt, J. R.: Surface influence upon vertical profiles in the atmospheric near-surface layer, Q. J. R. Meteorol. Soc., 106, 803–819, doi:10.1002/qj.49710645011, 1980.

Garrity, S. R., Meyer, K., Maurer, K. D., Hardiman, B. S., and Bohrer, G.: Estimating plot-level tree structure in a deciduous forest by combining allometric equations, spatial wavelet analysis and airborne lidar, Remote Sens. Lett., 3, 443–451, doi:10.1080/01431161.2011.618814, 2012.

Gent, P. R., Danabasoglu, G., Donner, L. J., Holland, M. M., Hunke, E. C., Jayne, S. R., Lawrence, D. M., Neale, R. B., Rasch, P. J., Vertenstein, M., Worley, P. H., Yang, Z.-L., and Zhang, M.: The community climate system model version 4, J. Climate, 24, 4973–4991, doi:10.1175/2011jcli4083.1, 2011.

Gough, C. M., Hardiman, B. S., Nave, L. E., Bohrer, G., Maurer, K. D., Vogel, C. S., Nadelhoffer, K. J., and Curtis, P. S.: Sustained carbon uptake and storage following moderate disturbance in a Great Lakes forest, Ecol. Appl., 23, 1202–1215, doi:10.1890/12-1554.1, 2013.

Grimmond, C. S. B. and Oke, T. R.: Aerodynamic properties of urban areas derived from analysis of surface form, J. Appl. Meteorol., 38, 1262–1292, doi:10.1175/1520-0450(1999)038<1262:apouad>2.0.co;2, 1999.

Hardiman, B. S., Bohrer, G., Gough, C. M., and Curtis, P. S.: Canopy structural changes following widespread mortality of canopy dominant trees, Forests, 4, 537–552, doi:10.3390/f4030537, 2013.

Harman, I. N. and Finnigan, J. J.: A simple unified theory for flow in the canopy and roughness sublayer, Bound.-Lay. Meteorol., 123, 339–363, doi:10.1007/s10546-006-9145-6, 2007.

Harman, I. N.: The role of roughness sublayer dynamics within surface exchange schemes, Bound.-Lay. Meteorol., 142, 1–20, doi:10.1007/s10546-011-9651-z, 2012.

Ivanov, V. Y., Bras, R. L., and Vivoni, E. R.: Vegetation-hydrology dynamics in complex terrain of semiarid areas: II. Energy-water controls of vegetation spatio-temporal dynamics and topographic niches of favorability, Water Resour. Res., 44, W03430, doi:10.1029/2006WR005595, 2008.

Jonckheere, I., Fleck, S., Nackaerts, K., Muys, B., Coppin, P., Weiss, M., and Baret, F.: Review of methods for in situ leaf area index determination: Part I. Theories, sensors and hemispherical photography, Agr. Forest Meteorol., 121, 19–35, doi:10.1016/j.agrformet.2003.08.027, 2004.

Lindroth, A.: Aerodynamic and canopy resistance of short-rotation forest in relation to leaf area index and climate, Bound.-Lay. Meteorol., 66, 265–279, doi:10.1007/bf00705478, 1993.

BGD

11, 16349–16389, 2014

LES of surface roughness parameters

K. D. Maurer et al.

Mahrt, L.: Computing turbulent fluxes near the surface: Needed improvements, Agr. Forest Meteorol., 150, 501–509, doi:10.1016/j.agrformet.2010.01.015, 2010.
Massman, W. J. and Weil, J. C.: An analytical one-dimensional second-order closure model of turbulence statistics and the Lagrangian time scale within and above plant canopies of arbitrary structure, Bound.-Lay. Meteorol., 91, 81–107, doi:10.1023/A:1001810204560, 1999.
Maurer, K. D., Hardiman, B. S., Vogel, C. S., and Bohrer, G.: Canopy-structure effects on surface roughness parameters: Observations in a Great Lakes mixed-deciduous forest, Agr. Forest Meteorol., 177, 24–34, doi:10.1016/j.agrformet.2013.04.002, 2013.
Medvigy, D., Wofsy, S. C., Munger, J. W., Hollinger, D. Y., and Moorcroft, P. R.: Mechanistic scaling of ecosystem function and dynamics in space and time: the Ecosystem Demography model version 2, J. Geophys. Res., 114, G01002, doi:10.1029/2008JG000812, 2009.
Mölder, M., Grelle, A., Lindroth, A., and Halldin, S.: Flux-profile relationships over a boreal forest – roughness sublayer corrections, Agr. Forest Meteorol., 98–99, 645–658, doi:10.1016/S0168-1923(99)00131-8, 1999.
Monin, A. S. and Obukhov, A. M.: Basic laws of turbulent mixing in the surface layer of the atmosphere, Tr. Geofiz. Inst. Akad. Nauk SSSR, 24, 163–187, 1954.
Moran, M. S.: A satellite-based approach for evaluation of the spatial distribution of evapotranspiration from agricultural lands, PhD thesis, University of Arizona, Tuscon, Arizona, USA., 223 pp., 1990.
Nakai, T., Sumida, A., Daikoku, K., Matsumoto, K., van der Molen, M. K., Kodama, Y., Kononov, A. V., Maximov, T. C., Dolman, A. J., Yabuki, H., Hara, T., and Ohta, T.: Parameterisation of aerodynamic roughness over boreal, cool- and warm-temperate forests, Agr. Forest Meteorol., 148, 1916–1925, doi:10.1016/j.agrformet.2008.03.009, 2008a.
Nakai, T., Sumida, A., Matsumoto, K., Daikoku, K., Iida, S., Park, H., Miyahara, M., Kodama, Y., Kononov, A. V., Maximov, T. C., Yabuki, H., Hara, T., and Ohta, T.: Aerodynamic scaling for estimating the mean height of dense canopies, Bound.-Lay. Meteorol., 128, 423–443, doi:10.1007/s10546-008-9299-5, 2008b.
Nakai, T., Sumida, A., Kodama, Y., Hara, T., and Ohta, T.: A comparison between various definitions of forest stand height and aerodynamic canopy height, Agr. Forest Meteorol., 150, 1225–1233, doi:10.1016/j.agrformet.2010.05.005, 2010.

BGD
11, 16349–16389, 2014

LES of surface roughness parameters

K. D. Maurer et al.

Nepf, H., Ghisalberti, M., White, B., and Murphy, E.: Retention time and dispersion associated with submerged aquatic canopies, Water Resour. Res., 43, W04422, doi:10.1029/2006WR005362, 2007.
Parker, G. G., Harding, D. J., and Berger, M. L.: A portable LIDAR system for rapid determination of forest canopy structure, J. Appl. Ecol., 41, 755–767, doi:10.1111/j.0021-8901.2004.00925.x, 2004.
Paulson, C. A.: The mathematical representation of wind speed and temperature profiles in the unstable atmospheric surface layer, J. Appl. Meteorol., 9, 857–861, doi:10.1175/1520-0450(1970)009<0857:TMROWS>2.0.CO;2, 1970.
Perrier, A.: Land surface processes: vegetation, in: Land processes in atmospheric general circulation models, edited by: P., E., Cambridge University Press, Cambridge, UK, 395–448, 1982.
Physick, W. L. and Garratt, J. R.: Incorporation of a high-roughness lower boundary into a mesoscale model for studies of dry deposition over complex terrain, Bound.-Lay. Meteorol., 74, 55–71, doi:10.1007/bf00715710, 1995.
Raupach, M. R. and Thom, A. S.: Turbulence in and above plant canopies, Annu. Rev. Fluid Mech., 13, 97–129, doi:10.1146/annurev.fl.13.010181.000525, 1981.
Raupach, M. R.: Drag and drag partition on rough surfaces, Bound.-Lay. Meteorol., 60, 375–395, doi:10.1007/bf00155203, 1992.
Raupach, M. R.: Simplified expressions for vegetation roughness length and zero-plane displacement as functions of canopy height and area index, Bound.-Lay. Meteorol., 71, 211–216, doi:10.1007/bf00709229, 1994.
Raupach, M. R., Finnigan, J. J., and Brunet, Y.: Coherent eddies and turbulence in vegetation canopies: The mixing-layer analogy, Bound.-Lay. Meteorol., 78, 351–382, doi:10.1007/BF00120941, 1996.
Santos, C., Lorite, I. J., Allen, R. G., and Tasumi, M.: Aerodynamic parameterization of the satellite-based energy balance (METRIC) model for ET estimation in rainfed olive orchards of Andalusia, Spain, Water Resources Management, 26, 3267–3283, doi:10.1007/s11269-012-0071-8, 2012.
Schaudt, K. J. and Dickinson, R. E.: An approach to deriving roughness length and zero-plane displacement height from satellite data, prototyped with BOREAS data, Agr. Forest Meteorol., 104, 143–155, doi:10.1016/S0168-1923(00)00153-2, 2000.

BGD
11, 16349–16389, 2014
LES of surface roughness parameters
K. D. Maurer et al.

Shaw, R. H., and Pereira, A. R.: Aerodynamic roughness of a plant canopy: A numerical experiment, Agr. Meteorol., 26, 51–65, doi:10.1016/0002-1571(82)90057-7, 1982.
Shaw, R. H., Denhartog, G., and Neumann, H. H.: Influence of foliar density and thermal-stability on profiles of reynolds stress and turbulence intensity in a deciduous forest, Bound.-Lay. Meteorol., 45, 391–409, doi:10.1007/BF00124010, 1988.
Tanner, C. B. and Pelton, W. L.: Potential evapotranspiration estimates by the approximate energy balance method of Penman, J. Geophys. Res., 65, 3391–3413, doi:10.1029/JZ065i010p03391, 1960.
Thom, A. S.: Momentum absorption by vegetation, Q. J. R. Meteorol. Soc., 97, 414–428, doi:10.1002/qj.49709741404, 1971.
Thomas, C. and Foken, T.: Flux contribution of coherent structures and its implications for the exchange of energy and matter in a tall spruce canopy, Bound.-Lay. Meteorol., 123, 317–337, doi:10.1007/s10546-006-9144-7, 2007a.
Thomas, C. and Foken, T.: Organised motion in a tall spruce canopy: temporal scales, structure spacing and terrain effects, Bound.-Lay. Meteorol., 122, 123–147, doi:10.1007/s10546-006-9087-z, 2007b.
Weligepolage, K., Gieske, A. S. M., and Su, Z.: Surface roughness analysis of a conifer forest canopy with airborne and terrestrial laser scanning techniques, Int. J. Appl. Earth Obs., 14, 192–203, doi:10.1016/j.jag.2011.08.014, 2012.
Wouters, H., De Ridder, K., and van Lipzig, N. P. M.: Comprehensive parametrization of surface-layer transfer coefficients for use in atmospheric numerical models, Bound.-Lay. Meteorol., 145, 539–550, doi:10.1007/s10546-012-9744-3, 2012.
Zheng, G. and Moskal, L. M.: Retrieving leaf area index (LAI) using remote sensing: theories, methods and sensors, Sensors, 9, 2719–2745, doi:10.3390/s90402719, 2009.
Zhou, Y., Sun, X., Ju, W., Wen, X., and Guan, D.: Seasonal, diurnal and wind-direction-dependent variations of the aerodynamic roughness length in two typical forest ecosystems of China, Terr. Atmos. Ocean. Sci., 23, 181–191, doi:10.3319/tao.2011.10.06.01(a), 2012.

Table 1. Description of simulation cases used for sensitivity analysis of roughness parameters derived from an LES over variable canopy layouts. Canopy structure was varied along four axes: (a) LAI, (b) vertical LAD profile, (c) canopy height, and (d) gap fraction.

Experiment	LAI ($m^2\,m^{-2}$)	LAD ($m^2\,m^{-3}$)	Height (m)	Gap fraction (%)
(a) LAI variation	1.0 2.6 3.2 3.7 4.2	Natural	21	0
(b) LAD profile variation	4.2	Lower Middle Natural Upper	21	0
(c) Canopy height variation	1.0	Natural	9 15 21 27	0
	4.2	Natural	9 15 21 27	0
(d) Gap fraction variation	1.0	Natural	27	0 10 25 35 50
	4.2	Natural	27	0 10 25 35 50

BGD
11, 16349–16389, 2014

Table 2. Results of a 3-way ANOVA to test any significance maximum canopy height (h_{max}), leaf area index (LAI), and gap fraction (GF) have on displacement height (d), roughness length (z_0), aerodynamic canopy height (h_a), or eddy-penetration depth (δ_e). P values listed in bold font indicate a significant effect.

Variable	3-way ANOVA p value		
	h_{max}	LAI	GF
d	**< 0.001**	0.065	0.370
z_0	0.290	0.227	0.918
h_a	**< 0.001**	**< 0.001**	**0.007**
δ_e	**< 0.001**	**0.001**	**0.004**

BGD
11, 16349–16389, 2014

BGD

11, 16349–16389, 2014

LES of surface roughness parameters

K. D. Maurer et al.

Table 3. 30 min block-averaged friction velocity (u_*) model evaluation against measured u_* for displacement height (d) and roughness length (z_0) calculated from various methods – Classical, Yearly Observed, Biometric, Raupach 94, and Nakai 08 – at US-UMB spanning the 2000–2011 growing seasons. We show the slope of the linear fit (Slope), the coefficient of determination (r^2), and the coefficient of variation (CV) between modeled and observed u_*.

Method		d (m)	z_0 (m)	Slope	r^2	CV (%)
Classical		14.0	2.10	1.63	0.80	28
Yearly Observed	Mean (2000–2011)	Variable		1.38	0.80	20
	Best (2008)	26.0	0.99	1.02	0.80	3
	Worst (2005)	18.3	1.99	1.57	0.80	27
Biometric		$f(h_{max}$, LAI, GF)		1.64	0.80	28
Raupach 94		$f(h, \Lambda)$		1.32	0.80	18
Nakai 08		$f(h, \rho_s$, LAI)		1.67	0.80	29

Table A1. Surface roughness parameters derived from an LES over variable canopy layouts. Canopy structure was varied along four axes: (a) LAI, (b) vertical LAD profile, (c) canopy height, and (d) gap fraction.

Experiment	LAI ($m^2\,m^{-2}$)	LAD ($m^2\,m^{-3}$)	Height (m)	Gap fraction	d (m)	z_0 (m)	d/h	z_0/h	λ	h_a (m)	δ_e (m)
(a) LAI variation	1.0	Natural	21	0 %	14.2	2.6	0.67	0.12	0.38	20.9	13.1
	2.6				13.7	3.1	0.65	0.15	0.41	21.1	11.0
	3.2				16.5	1.3	0.79	0.06	0.27	21.1	10.7
	3.7				7.6	4.0	0.36	0.19	0.29	21.2	9.9
	4.2				16.0	1.2	0.76	0.06	0.24	21.1	10.2
(b) LAD profile variation	4.2	Lower	21	0 %	13.6	1.7	0.65	0.08	0.24	20.7	12.6
		Middle			8.8	5.7	0.42	0.27	0.55	19.1	8.2
		Natural			16.0	1.2	0.76	0.06	0.24	21.1	10.2
		Upper			13.8	2.8	0.66	0.14	0.38	21.2	10.2
(c) Canopy height variation	1.0	Natural	9	0 %	4.4	0.8	0.49	0.09	0.17	9.3	7.1
			15		3.6	3.5	0.24	0.23	0.31	15.0	10.1
			21		14.2	2.6	0.67	0.12	0.38	20.9	13.1
			27		20.1	2.5	0.74	0.09	0.36	26.9	15.8
	4.2	Natural	9	0 %	3.7	2.0	0.41	0.22	0.35	9.4	6.3
			15		8.7	2.5	0.58	0.17	0.38	15.2	7.9
			21		16.0	1.2	0.76	0.06	0.24	21.1	10.2
			27		20.1	2.9	0.75	0.11	0.41	27.1	11.9
(d) Gap fraction variation	1.0	Natural	27	0 %	20.1	2.5	0.74	0.09	0.36	26.9	15.8
				10 %	19.8	2.2	0.73	0.08	0.31	26.8	17.5
				25 %	18.5	3.2	0.69	0.12	0.39	26.8	18.2
				35 %	17.9	2.4	0.66	0.09	0.27	26.7	19.2
				50 %	18.7	1.8	0.69	0.07	0.23	26.7	20.2
	4.2	Natural	27	0 %	20.1	2.9	0.75	0.11	0.41	27.1	11.9
				10 %	20.4	2.7	0.76	0.10	0.42	27.0	13.0
				25 %	18.7	2.8	0.69	0.11	0.34	27.0	14.4
				35 %	19.1	2.4	0.71	0.09	0.30	26.9	15.8
				50 %	14.4	4.0	0.53	0.15	0.32	26.9	17.3

BGD
11, 16349–16389, 2014

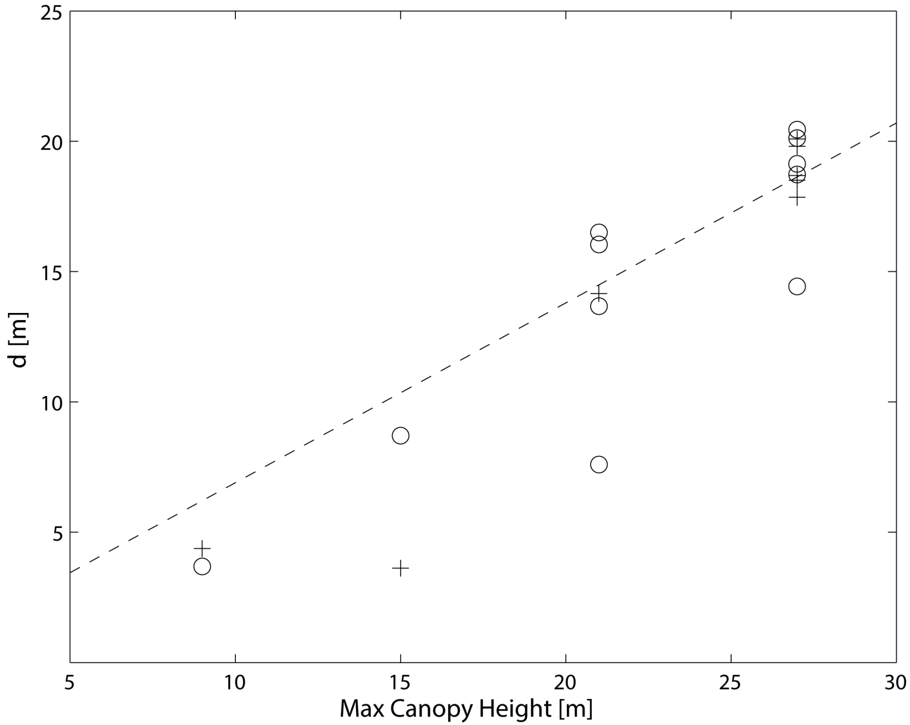

Figure 1. LES domain-averaged d vs. maximum canopy height. Crosses and circles correspond to leaf-off ($LAI = 1.0\,m^2\,m^{-2}$) and leaf-on ($LAI > 1.0\,m^2\,m^{-2}$) conditions, respectively. Best-fit line (forced through [0,0]) shown as dashed line ($d = 0.69 h_{max}$).

BGD
11, 16349–16389, 2014

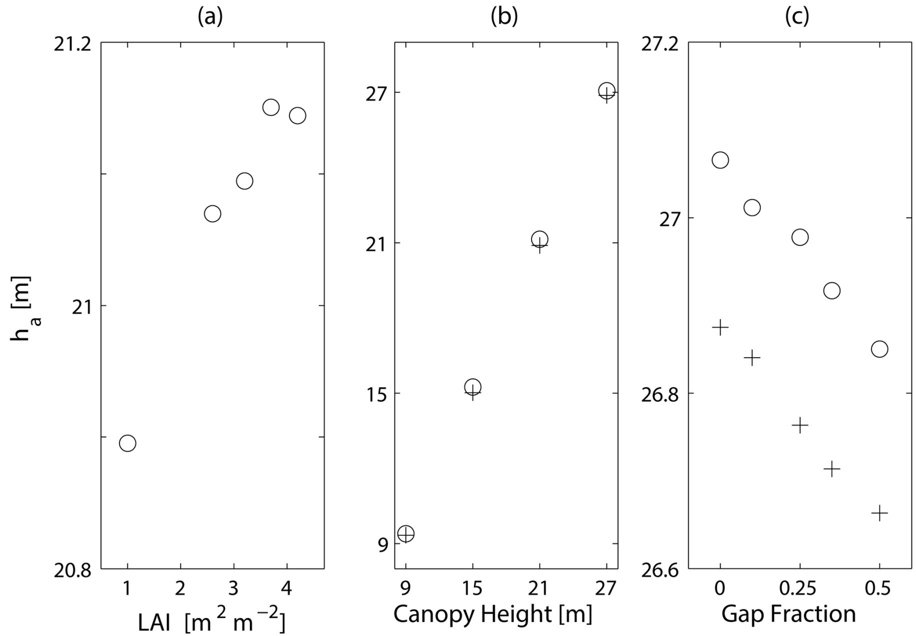

Figure 2. LES domain-averaged aerodynamic canopy height (h_a) vs. **(a)** leaf area index (LAI), **(b)** canopy height (h_{max}), and **(c)** gap fraction (GF). For **(b)** and **(c)**, crosses and circles correspond to leaf-off and peak-LAI conditions, respectively.

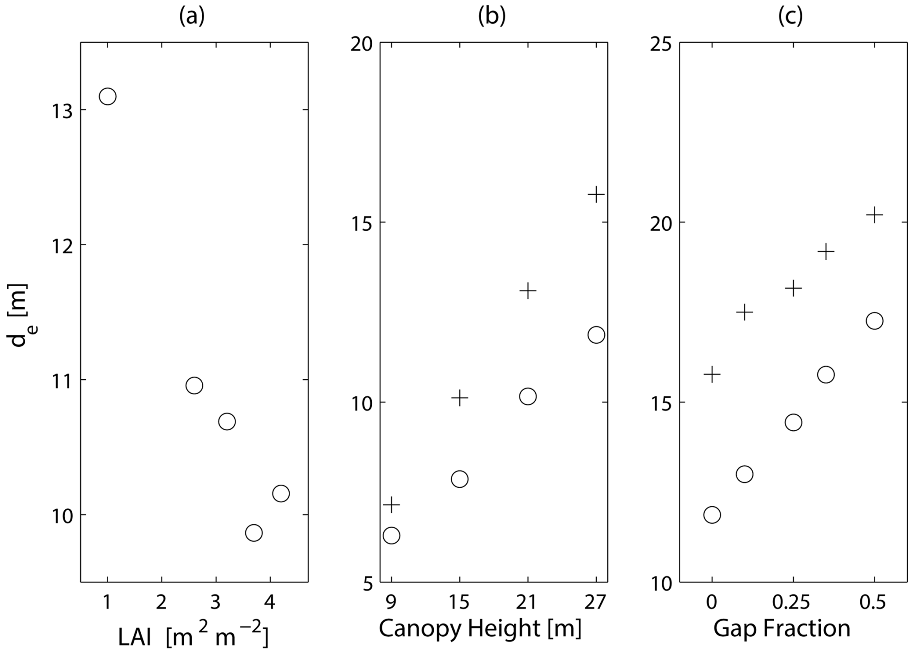

Figure 3. LES domain-averaged eddy-penetration depth (δ_e) vs. **(a)** leaf area index (LAI), **(b)** canopy height (h_{max}) and **(c)** gap fraction (GF). For **(b)** and **(c)**, crosses and circles correspond to leaf-off and peak-LAI conditions, respectively.

BGD
11, 16349–16389, 2014

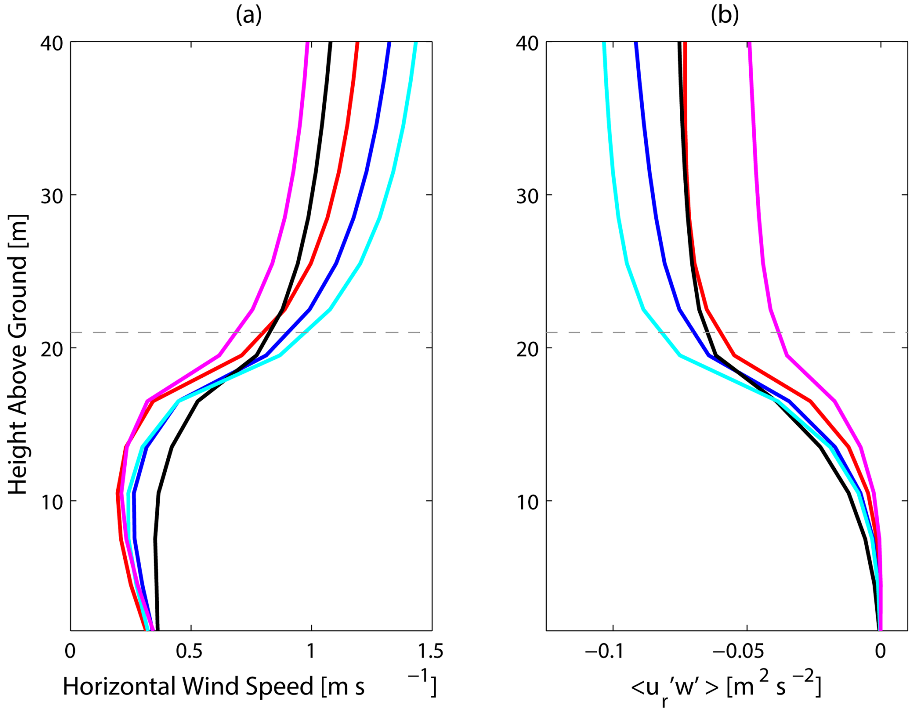

Figure 4. (a) Horizontal wind profiles and **(b)** Reynold's stress for LAI = 1.0 $m^2 m^{-2}$ (black), LAI = 2.6 $m^2 m^{-2}$ (blue), LAI = 3.2 $m^2 m^{-2}$ (cyan), LAI = 3.7 $m^2 m^{-2}$ (magenta), and LAI = 4.2 $m^2 m^{-2}$ (red). Canopy height shown as horizontal gray line.

BGD
11, 16349–16389, 2014

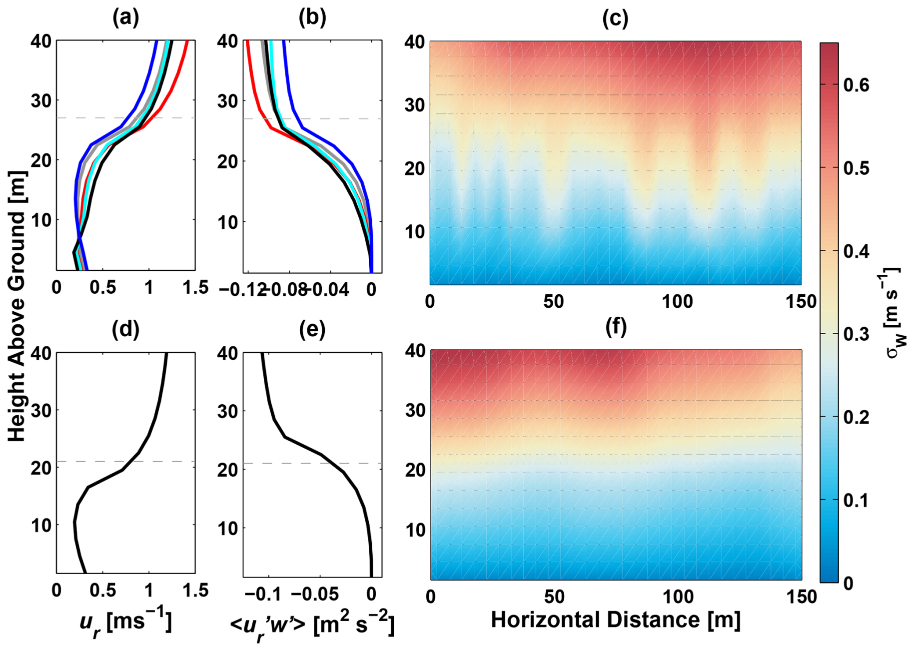

Figure 5. (a, d) Horizontal wind profiles, **(b, e)** Reynold's stress, and **(c, f)** wind and SD of vertical wind for horizontally heterogeneous – gap fractions of 0 % (blue), 10 % (gray), 25 % (red), 35 % (cyan), and 50 % (black) – and homogenous canopies, respectively. Canopy height cross-section shown as solid gray line in **(c)** and **(f)**.

BGD
11, 16349–16389, 2014

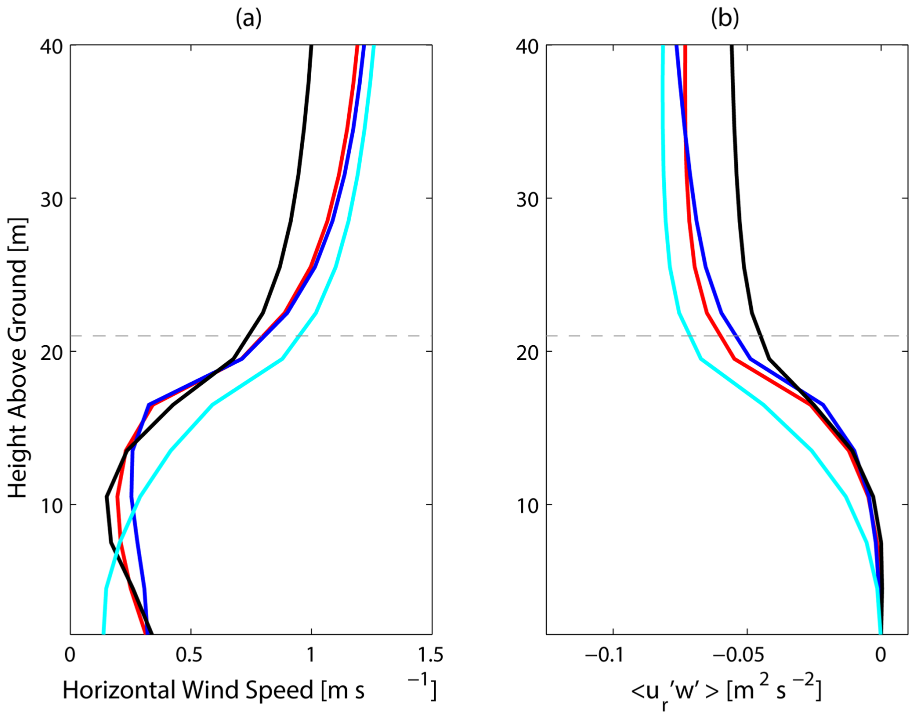

Figure 6. (a) Horizontal wind profiles and **(b)** Reynold's stress for "Lower" (cyan), "Middle" (black), "Upper" (blue), and "Natural" (red) LAD profiles. Canopy height shown as horizontal gray line.

BGD
11, 16349–16389, 2014

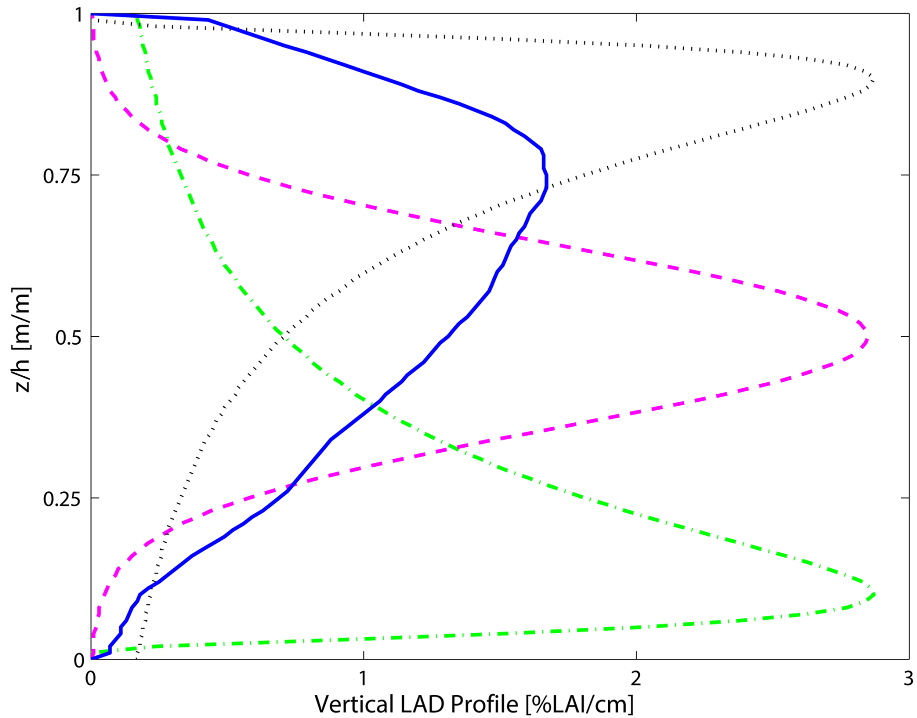

Figure A1. "Lower" (-·-) green; "Middle" (- -) magenta; "Upper" (···) black; and "Natural" (solid line) blue (mean observed in the US-UMB forest plot), vertical LAD profiles used in virtual canopies for RAFLES simulations.

BGD
11, 16349–16389, 2014

Title Page
Abstract | Introduction
Conclusions | References
Tables | Figures
Back | Close
Full Screen / Esc
Printer-friendly Version
Interactive Discussion

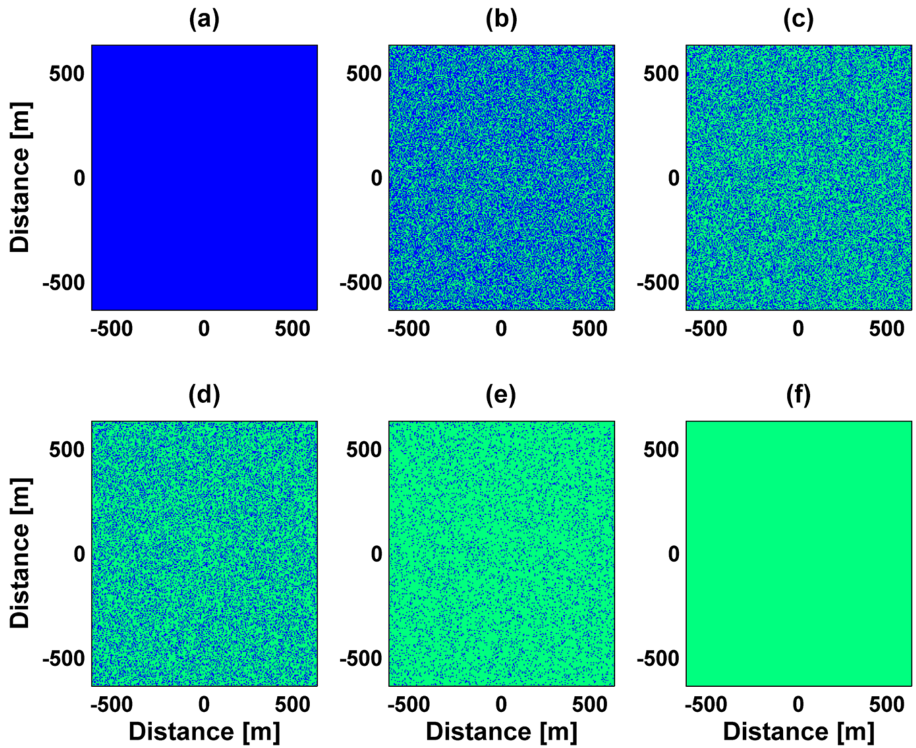

Figure A2. Height maps for varied plot-level gap fractions: **(a)** 100 %, **(b)** 50 %, **(c)** 35 %, **(d)** 25 %, **(e)** 10 %, and **(f)** 0 %. Here, gap fraction refers to the percentage of the canopy described by h_L ($h = 9$ m, blue) as opposed to h_H ($h = 27$ m, green).